Available online at www.sciencedirect.com
SCIENCE DIRECT®
Tectonophysics 379 (2004) 139–157
TECTONOPHYSICS
www.elsevier.com/locate/tecto

Burial and thermal history of the West Bashkirian sedimentary basins

Yu.I. Galushkin[a,*], G.E. Yakovlev[b]

[a] Earth Sciences Museum, Moscow State University, Vorobievy Gory, 119899 Moscow, Russia
[b] Geology Faculty, Moscow State University, Vorobievy Gory, 119899 Moscow, Russia

Received 18 October 2002; accepted 15 October 2003

Abstract

The GALO system is applied to the numerical reconstruction of burial and thermal histories of the West Bashkirian lithosphere from the Riphean to the present. An analysis of the variation in tectonic subsidence of the basin during its development is utilized to estimate approximately the mantle heat flow variations. Our variant of basin evolution suggests that after cooling in the Early Riphean, the rather weak thermal reactivations have not led to considerable heating of the lithosphere in the study region. Surface heat flow decreased from relatively high values in the Early Riphean (60–70 mW/m^2 in the eastern area and 40–50 mW/m^2 in the western part) to present-day values of 32–40 mW/m^2. In spite of the relatively low temperature regime of the basin as a whole, a syn-rifting deposition of more than 10 km of limestone, shale and sandstone in the Riphean resulted in rather high temperatures (180–190 °C) at the base of present-day sedimentary blanket in the eastern area. In agreement with the observed data, computed present-day heat flow through the sediment surface increases slightly from 32 to 34 mW/m^2 near the west boundary of the region to 42 mW/m^2 near the boundary of the Ural Foldbelt, whereas the heat flow through the basement surface decreases slightly from 28–32 to 24–26 mW/m^2 in the same direction. The mantle heat flow is only 11.3–12.7 mW/m^2, which is considerable lower than mean heat flow of the Russian Platform (16–18 mW/m^2) and comparable with the low heat flow of Precambrian shields.

Keywords: West Bashkiria; Thermal and burial reconstruction; Basin modeling; Heat flow; Tectonic subsidence; Strength of the lithosphere

1. Introduction

The study region includes the West Bashkirian sedimentary basins and adjacent areas of the South Urals (Fig. 1). The main two aspects determine an increased interest of geologists and geophysics to this region. The first relates to oil and gas prospecting of the Riphean and Vendian deposits in the Bashkiria (Aliev et al., 1977; Belokon et al., 1996; Masagutov et al., 1997). The second aspect concerns anomalous low heat flow in the region that has been analyzed in many papers (Salnikov, 1984; Salnikov and Golovanova, 1990; Khutorskoy et al., 1993; Kukkonen et al., 1997). Application of the GALO system for basin modeling enables considering the above aspects. The numerical reconstruction of burial and thermal histories of the West Bashkirian basins, presented in the paper, can be helpful for oil and gas prospecting of the

* Corresponding author.
E-mail address: dubinin@museum.msu.ru (Y.I. Galushkin).

0040-1951/$ - see front matter © 2003 Elsevier B.V. All rights reserved.
doi:10.1016/j.tecto.2003.10.019

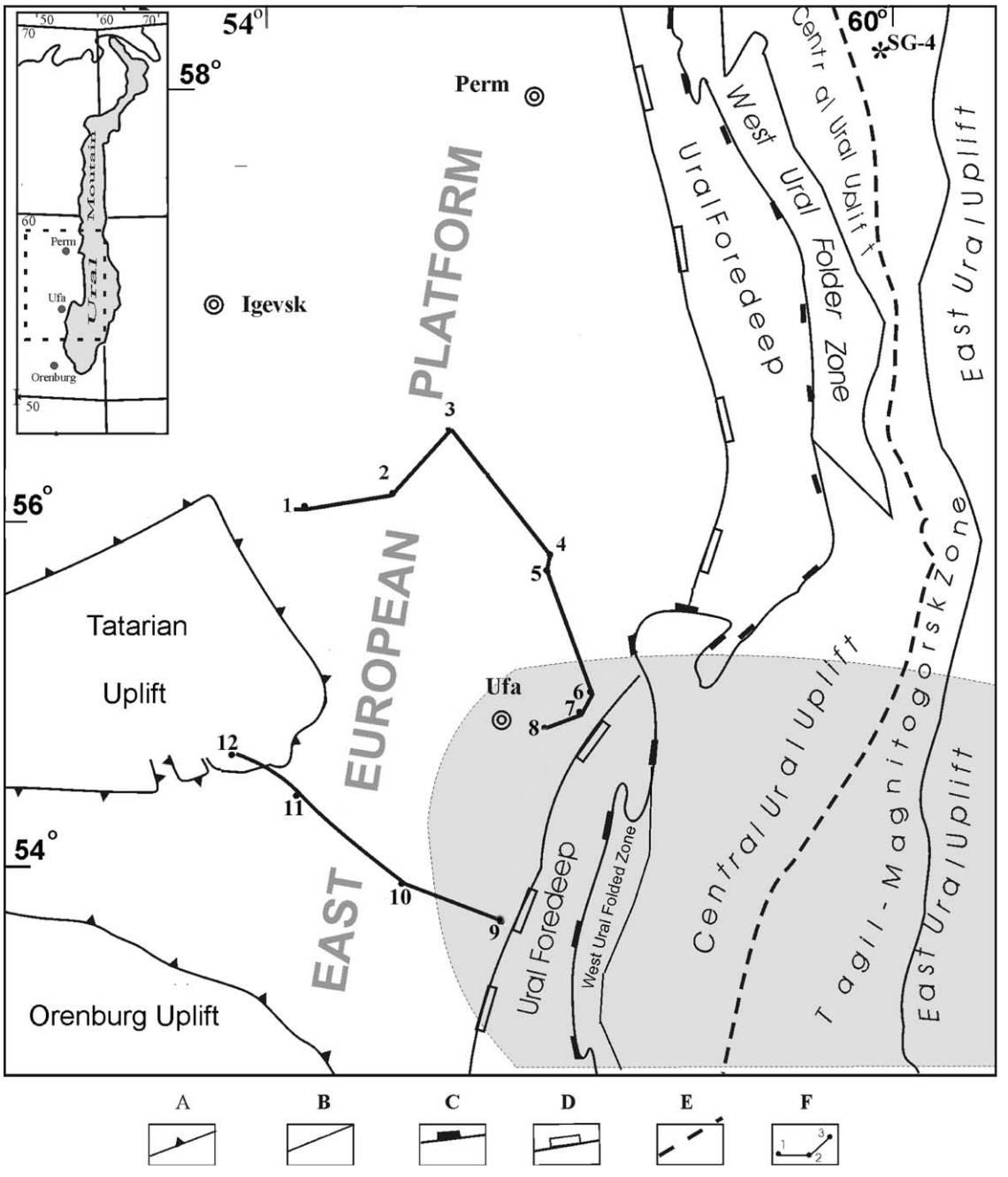

Fig. 1. Generalized location map and main tectonic structures of the South Urals region, showing modeled wells and profiles in the West Baskirian. (Ruzhenzev, 1976; Belokon et al., 1996; Maslov et al., 1997). (A) main tectonic structure of the West Baskirian, (B) boundaries of the West Ural Folded Zone and the East Ural Uplift, (C and D) western and eastern boundaries of the Ural Foredeep, (E) the Main Ural Fault, (F) profiles and wells considered in the paper. Shaded area shows approximately the region of low heat flow after (Smirnov, 1980). The numbers correspond the following wells: 1 = Arlanskaya, 2 = Koltasinskaya, 3 = Yugomashskaya, 4 = Severo – Kushkulskaya, 5 = Kushkulskaya, 6 = Yuzhno – Taftimanovskaya-1, 7 = Yuzhno – Taftimanovskaya-2, 8 = Kabakovskaya, 9 = Akhmerova, 10 = Kipchackskaya, 11 = Aslykulskaya, 12 = Morozovskaya. Profile 1 crosses the wells 1 – 8 and the profile 3 crosses the wells 9 – 12.

deep Riphean and Vendian horizons in the region (Belokon et al., 1996). In addition, the fulfilled basin modeling has the advantage that heat transition in basin is considered taking into account the variation in porosity, heat conductivity, heat capacity and volume heat generation of sedimentary rocks with depth and rock lithology. The demonstrated comparison of the computed and measured distributions of temperature and heat flow with depth in the regions with considerable effect of paleoclimatic factor is of particular interest.

The studied region have developed initially as intracratonic basins similar to avlakogene, evolved as intracratonic half-structures after opening of the Urals paleoocean in the Early Ordovician and were transformed into margin basins of the East European Platform during the Ordovician (Maslov et al., 1997). After a short discussion of the GALO system for basin modeling, the paper deals with database for numerical reconstruction of thermal and burial histories. The reliability of our reconstructions is based on geological and geophysical information about the structure evolution of the region including some geological sections constructed with the aid of borehole and seismic data. Temperature measurements in more than 30 boreholes at depths of more than 1 km, carried out with detailed consideration of climatic factor, are used as input and control data. The corresponding updated version of the GALO system (Galushkin, 1997) allows consideration of climatic factor within the framework of basin modeling system for actual lithological section of the area under analysis and with detailed reconstructions of paleoclimatic curve for the last 1–3 My (Velichko, 1987, 1999).

The most important obtained result is a complete temperature history reconstruction of the sedimentary cover sequences and the underlying lithosphere of the region, which is more accurate than those obtained with commonly used simple modeling techniques (Salnikov, 1984; Salnikov and Golovanova, 1990; Khutorskoy et al., 1993; Kukkonen et al., 1997). Combined analysis of the heat transfer in the sedimentary blanket and the underlying lithosphere allows analysis of the variations in tectonic subsidence of the basin to be utilized for approximate estimate of changes in the mantle heat flow during the basin history. As a whole, our modeling assumes rather moderate thermal regime of the basin's lithosphere during the post-rifting stage of its development with surface heat flow ranging between 40 and 50 mW/m^2. Such regime results in relatively low maturation level of Riphean and Vendian organic matter in present-day sections of the region aside from the deeply buried horizons. Tectonic analysis utilized in our modeling suggests isostatic response of the lithosphere on load. Isostasy and strength of the lithosphere are discussed in the last parts of the paper. We believe that there is little probability that the basin's lithosphere is far from isostatic state because of rather large horizontal size of the sedimentary load and the presence of relatively weak rheological layers within the crust. Only the relatively short time of the Ural Orogen collision could be an exception. Our numerical estimate of the maturity level of Riphean and Vendian organic matter, reflecting the integral thermal history of buried rocks is in agreement with the existing geochemical data (Galushkin et al., 2004).

2. Geological background

The West Bashkirian region includes several Riphean sedimentary basins and is adjacent to the complex tectonic region of the Urals Orogen (Fig. 1). This Orogen is a folded nappe structure formed in the Devonian–Triassic in situ of paleoceanic basins as result of the East European Platform collision with the East Ural's micro-continents and the Sibirian–Kazkhstan Caledonian continent (Ruzhenzev, 1976). The following tectonic structures can be observed in the region from the West to the East (Fig. 1): the East European Platform (EEP), the Ural Foredeep, the West Ural Foldbelt, the Central Ural Uplift, the Tagil–Magnitogorsk (T–M) Zone, the East Ural Uplift and Depression, the Trans-Ural Uplift and Kazakhstan Folded Zone. Only three of the above cited structures are considered in our study: the East European Platform, the Urals Foredeep and the T–M Zone. The last includes oceanic and back-arc complex of the Paleozoic age and is bounded by the Main Uralian Fault in the West. This Fault separates the back-arc rocks of the M–T Zone from the West Ural Foldbelt and outcrops the Riphean and Vendian metamorphic basement of the East European Platform in the Central Urals Uplift. The eastward dip of the Main Uralian Fault is clearly displayed by seismic profiling

Table 1
Main evolution stages of the sedimentary basin near Akhmerova well (West Bashkiria)

N	Evolution stages	Geological time (Ma)	Depth (m)	Lithology cl:sn:ls:an	Surface paleo-temperature (°C)
1	interrupt.	0–100	0	–	5–24
2	erosion	100–253	400	–	12–24
3	sedim.	253–258	0–110	10:90:00:00	10–12
4	sedim.	258–352	110–1330	00:00:73:27	5–16
5	sedim.	352–387	1330–1640	03:10:87:00	16
6	erosion	387–590	300	–	15–16
7	sedim.	590–660	1640–3240	17:83:00:00	15
8	erosion	660–680	300	–	15
9	sedim.	680–1050	3240–3640	22:55:23:00	13–15
10	sedim.	1050–1160	2640–5040	30:40:30:00	12–13
11	erosion	1160–1350	600	–	11–12
12	sedim..	1350–1650	5040–14500	20:20:60:00	10–11

Column "depth" shows the present-day depths of the bottom and roof of sedimentary layers or otherwise the erosion amplitude.
sedim.—sedimentation, interrupt.—interruption in sedimentation, an—anhydrite, cl—clay and shale, lm—limestone, sl—siltstone, sn—sandstone.

in the central and southern Urals (Juchlin et al., 1995; Echler et al., 1997). Tectonic activity in the Middle and South Urals deceased since the Late Permian (Ruzhenzev, 1976; Maslov et al., 1997).

According to geological data (Aliev et al., 1977; Belokon et al., 1996; Maslov et al., 1997), the Riphean–Vendian basins in the West Bashkiria have developed initially as intracratonic basins similar to avlakogene. They evolved as intracratonic half-structures only after opening of the Urals paleoocean in the Early Ordovician and were transformed into margin basins of the East European Platform during the Ordovician (Maslov et al., 1997). The position of some Low Riphean rifting axis correspond probably to maximal thickness of Riphean–Vendian sedimentary complex within the Urals Foredeep (Fig. 1; Belokon et al., 1996; Masagutov et al., 1997; Maslov et al., 1997). Thus, sedimentation in the Low and Middle Riphean took place in the setting similar to that of continental rifting and is accompanied by heating and extension of the basin lithosphere. Gabbro-diabase samples of 1030–1450 Ma found in the Low and Middle Riphean deposits (Belokon et al., 1996) suggest a possible thermal reactivation of the region at that time. Shallow-sea terrigenous and carbonate sediments were accumulated during the middle and late phases of the Early Riphean. The Riphean–Vendian sedimentation ranged from shallow-sea to continental (Aliev et al., 1977; Belokon et al., 1996; Masagutov et al., 1997; Maslov et al., 1997).

The Cambrian sediments are absent in the Urals and adjacent areas. All the time including the Ordovician and the Early Cambrian is characterized by erosion or interruption in deposition (Table 1; Fig. 2b,f) resulted from some uplift of the region, which took place just before and during the opening of the Urals paleoocean in the Ordovician–Early Devonian

Fig. 2. Burial and thermal histories of the West Bashkirian basins near the Yugomashskaya (a–e) and Akhmerova (f–i) wells, derived from basin modeling. (a) Paleoclimate history of the region generalized for the last 5 My (Frakes, 1979; Velichko, 1987). (b and f) Burial and thermal histories of the sedimentary section: Solid lines—base of the sedimentary layers; long dashed lines—isotherms. (c and g) Computed variations in the heat flow during the basin evolution. The difference between the heat flows through the surfaces of the basement (dashed line) and through the sediment surface (solid line) is mainly due to radiogenic heat generation in sediments. (d and h) Tectonic subsidence of the basement surface calculated in the local isostasy approach by removing sediment and water load (solid line) and by consideration of time variations in density profile of the basement (dashed line, see text). TACi is the *i*th thermal reactivations of the basin lithosphere; EXT is the period of its extension (see text). (e and i) Evolution of the thermal regime of the basin lithosphere. Long dashed lines are isotherms. The "moho" line is the base of the crust. The "phase transition" line is the location of "pyroxene peridotite– garnet peridotite" compositional transition in the mantle (Forsyth and Press, 1971).

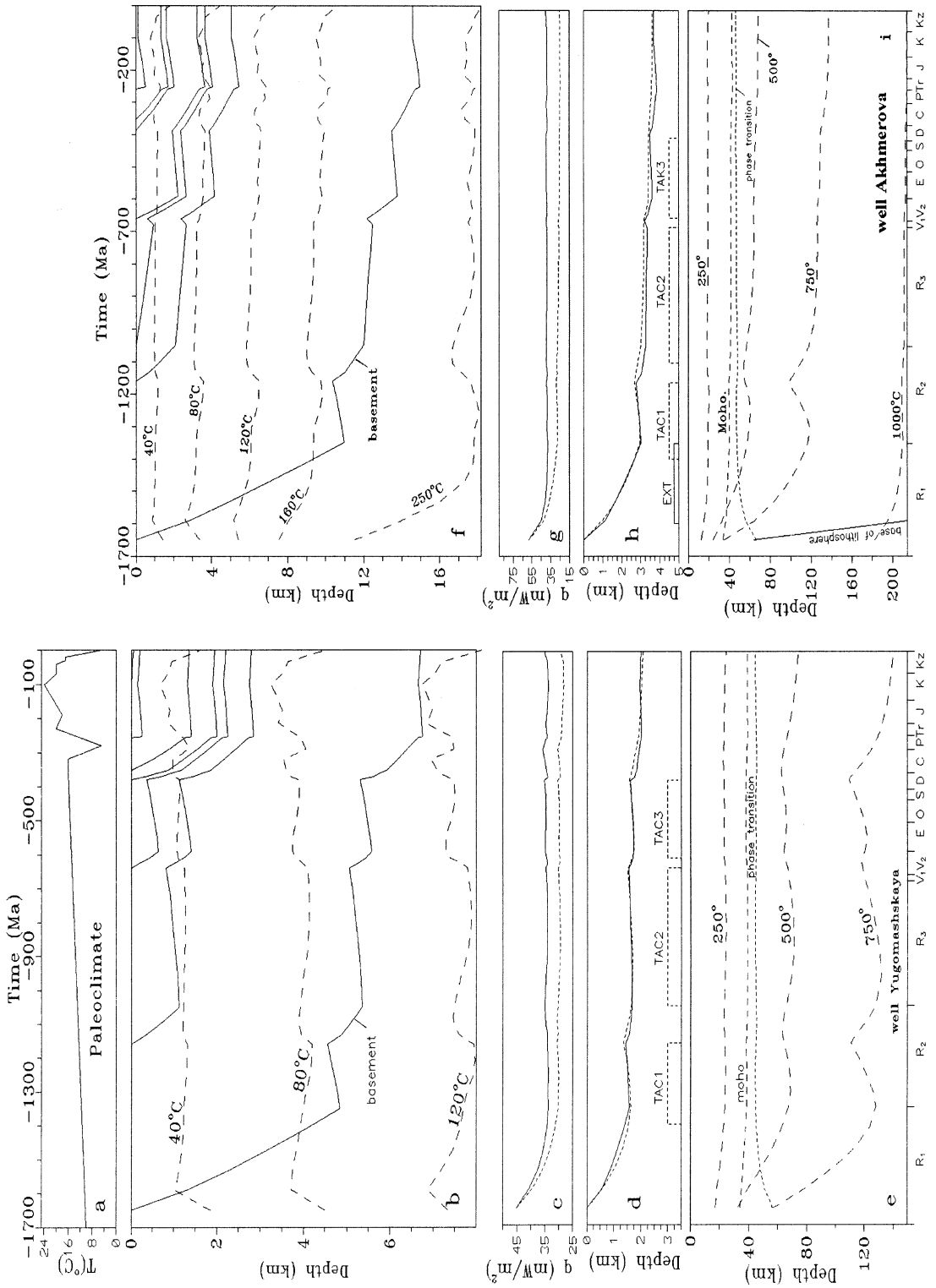
Time (Ma)
-1700
-1300
-900
-500
-100
T(°C)
a
Paleoclimate
Depth (km)
40°C
80°C
120°C
basement
b
q (mW/m²)
c
TAC1
TAC2
TAC3
d
moho
phase transition
250°
500°
750°
well Yugomashskaya
e
R1
R2
R3
V1V2
E
O
S
D
C
PTr
J
K
Kz
Time (Ma)
-1700
-1200
-700
-200
40°C
80°C
120°C
160°C
250°C
basement
f
g
EXT
TAC1
TAC2
TAK3
h
Moho
250°
500°
750°
1000°C
base of lithosphere
well Akhmerova
i

(Maslov et al., 1997). The small erosion amplitude (less than 300 m) suggests a weak thermal effect of the paleoocean opening on the West Bashkirian lithosphere in this time that could be linked with considerable distance between the region and the paleo-spreading centers or/and with limited amplitude of the ocean opening at that time (Didenko et al., 2001).

The next stage of the region development coincides with the closing of the Urals paleoocean in the Middle, the Upper Devonian and the Carboniferous which was accompanied by subduction of the oceanic or back-arc crust to the east along the Magnitogorsk volcanic arc (Juchlin et al., 1995; Echler et al., 1997; Didenko et al., 2001). Shallow-water limestones were deposited during over all of this period (Aliev et al., 1977; Belokon et al., 1996; Masagutov et al., 1997). Considerable admixture of terrigenous rocks appeared here only at the end of the Permian, when the margin of the East European Platform came into contact with the island arc block along the Main Urals Fault. Collision of the East European Platform with the East Urals micro-continents and the Sibirian–Kazkhstan Caledonian continent resulted in Urals Orogen of length of more than 3000 km (Ruzhenzev, 1976; Didenko et al., 2001). The crust blocks of ophiolitic and island arc rocks are located at present time just to the east of the Main Urals Fault (Fig. 1; Ruzhenzev, 1976; Kukkonen et al., 1997; Doring et al., 1997; Didenko et al., 2001). All over the time after collisions the West Bashkirian basins are characterized by little erosion (100–300 m) or interruption in deposition (Table 1; Fig. 2b,f).

3. Numerical reconstruction of burial and thermal histories of the West Bashkirian basins

The GALO system for basin modeling is used to restore numerically the burial and thermal histories of the West Bashkirian basins from Riphean to present time. The reconstructions are based on geological information about structure and development of the region, geological sections, burial and seismostratigraphic data, measurements of deep temperatures and heat flow in present-day sections and analysis of variations in tectonic subsidence of the basin.

3.1. Modeling principles

The algorithms and principals of the GALO package for basin modeling applied for thermal analysis are described in detail in Makhous et al. (1997) and Galushkin (1997) and only the main factors are touched upon here. The basin modeling is carried out by numerical solution of one-dimensional non-steady heat transfer equation in compacting domain with moving boundaries and thermophysical attributes of rocks changing with depth and time. For temperature calculation, the temperature corresponding to paleoclimate of the region at that time is taken at the surface of z-domain,. The steady temperature was maintained at the base of the domain. In our modeling, it ranged from 900 to 1000 °C. Its determination together with the construction of the initial and boundary conditions and the finite-difference scheme for solution of the heat transfer equation have been considered in the work of Makhous et al. (1997) and Galushkin (1997). It can be noted only that in the modeling the dz-steps did not exceed 20 m at the surface of the computed domain and increased up to 1–2 km at its base (at $z \approx 200$ km).

Similar to other modeling systems (Ungerer et al., 1990; Welte et al., 1997), the GALO system considers several processes typical for sedimentary basin formation: deposition and compaction of porous sediments with variable rates, erosion and interruption in sedimentation (nondeposition), change in thermophysical attributes of rocks with lithology, depth and temperature, the temperature dependence of water and matrix heat conductivity and others (Makhous et al., 1997; Galushkin, 1997; Galushkin et al., 1999). In addition, the GALO system allows consideration of some specific features in the reconstruction of the West Bashkirian basins. First of all, the system simulates the heat transfer in the sedimentary section and the underlying lithosphere and asthenosphere up to depth of 200–220 km with consideration of latent heat effect of fusion during high-temperature stages of the basin evolution in the Riphean. Secondly, our modeling involves analysis of the basement tectonic subsidence during basin evolution to estimate the sequence and amplitude of tectonic–thermal events, which could occur during the basin evolution (Makhous et al., 1997; Galushkin et al., 1999; Makhous and Galushkin, 2003). The variations in

the basement tectonic subsidence are computed in our modeling by two independent methods. The first calculates the response of the lithosphere caused by removing of water and sediments load:

$$Z_{\mathrm{Ts}}(t) - Z_{\mathrm{Ts}}(0) = \frac{\rho_{\mathrm{a}} - \rho_{\mathrm{s}}(t)}{\rho_{\mathrm{a}}} S(t) + \frac{\rho_{\mathrm{a}} - \rho_{\mathrm{w}}}{\rho_{\mathrm{a}}} [Z_{\mathrm{w}}(t) - Z_{\mathrm{w}}(0)]$$

where: t is the current time, $t=0$ is the time of the basin initiation, Z_{w} is the water column paleodepth, $Z_{\mathrm{Ts}}(t)$ is the tectonic subsidence amplitude at time t, $S(t)$ is the total thickness of sedimentary cover, ρ_{a} and ρ_{w} are the asthenosphere and water densities, $\rho_{\mathrm{s}}(t)$ is the average density in the sediment column:

$$\rho_{\mathrm{s}}(t) = \frac{\int_0^{S(t)} \rho_s(Z,t)\mathrm{d}Z}{S(t)}$$

The porosity $\varphi(Z,t)$ and the density $\rho_{\mathrm{s}}(Z,t) = \rho_{\mathrm{m}}(Z,t)[1-\varphi(Z,t)] + \rho_{\mathrm{w}}\varphi(Z,t)$ of rocks within the sedimentary column and weight of the column are computed to determine the average density $\rho_{\mathrm{s}}(t)$ at every time of the basin evolution. Above, ρ_{m} is the matrix density of the rock at depth of Z and time t. Estimated variations in the basement tectonic subsidence are shown in Fig. 2d and h by solid lines. In the second method, tectonic subsidence is determined from the time variations in density distribution with depth within the basement (Makhous et al., 1997):

$$Z_{\mathrm{T_b}}(t) - Z_{\mathrm{T_b}}(0) = \frac{G(t) - G(0)}{\rho_{\mathrm{a}} g}$$

Here, g is the gravity acceleration, G, is the weight of the basement column of fixed length l_{o},

$$G(t) = g \int_0^{l_{\mathrm{o}}} \rho_{\mathrm{l}}(Z,t)\mathrm{d}Z$$

The weight is calculated at every time step of modeling. The density of lithosphere rocks $\rho_{\mathrm{l}}(Z,t)$ is a function of temperature $T(Z,t)$ and pressure $P(Z,t)$:

$$\rho_{\mathrm{l}}(Z,t) = \rho_0(Z,t)[1 - \alpha T(Z,t) + \beta P(Z,t)]$$

where α is the thermal expansion coefficient, β is the isothermal compressibility of the rock, $\rho_{\mathrm{o}}(Z,t)$ is the density at the standard conditions $P=1$ atm and $T=20$ °C. The parameter ρ_{o} reflects variation in the rock type versus depth (crust, mantle, "granitic" or "basaltic" rock, the compositional transition in the mantle (Forsyth and Press, 1971), and the possible changes in the density distribution within the basement due to basement stretching (Fig. 2). The effect of change in the depth of the compositional transition boundary (plagioclase peridotite into garnet peridotite) on the tectonic subsidence amounts to the first hundreds of meters. Another compositional transition (pyroxene peridotite to plagioclase peridotite) is not taken into account often, because it occurs within the crust, but not in the mantle according to pressure–temperature conditions (Forsyth and Press, 1971). This density distribution in the lithosphere column up to depth of 200–220 km (depth of isostatic compensation in our modeling) is calculated at every time step of the basin development, including times of thermal activation and extension of the basement. The corresponding variations in the basement tectonic subsidence are shown in Fig. 2d and h by dashed lines. Both of the tectonic curves (solid and dashed) must coincide at local isostasy response of the basin lithosphere on internal and external load. The assumed thermal reactivation or extension of the lithosphere changes density distribution in the basement. An amplitude and duration of the event are chosen to ensure coinciding the dashed tectonic line with the solid, provided that the chosen parameters do not contradict to available geological and geophysical information about structure and evolution of the region (Fig. 2d and h; Makhous et al., 1997; Makhous and Galushkin, 2003). A special modification of the GALO system is applied to correct the thermal history of the basins during climate variations in the Pliocene–Holocene when permafrost could arise or degrade (Galushkin, 1997).

3.2. Initial data for modeling

The lithological sections of the sedimentary blanket utilized in our modeling are constructed on the basis of bore-hole data for depths of less than 5 km (Salnikov and Golovanova, 1990; Aliev et al., 1977; Belokon et al., 1996; Masagutov et al., 1997), and on the ground of seismic data for greater depth (Working Scheme, 1981; Frolovich et al., 1988). As a whole, the sedimentary rocks in the West Bashkirian basins are presented by shale, sandstone, and limestone with rare

Table 2
Petrophysical parameters of sedimentary rocks in the Akhmerova area (West Bashkiria)

N	$\varphi(0)$	b (km)	K_m (W/m °C)	Al (°C^{-1})	C_v (Mj/m^3 °K)	ρ_m (g/cm^3)	A (μW/m^3)
1	–	–	–	–	–	–	–
2	–	–	–	–	–	–	–
3	0.454	2.07	3.91	0.0027	2.826	2.65	0.963
4	0.554	1.67	3.50	0.0016	2.529	2.63	0.481
5	0.590	1.92	3.04	0.0007	2.726	2.70	0.691
6	–	–	–	–	–	–	–
7	0.487	2.49	3.72	0.0025	2.780	2.66	1.051
8	–	–	–	–	–	–	–
9	0.551	2.21	3.32	0.0018	2.713	2.67	1.068
10	0.586	2.14	3.07	0.0014	2.650	2.68	1.151
11	–	–	–	–	–	–	–
12	0.600	2.21	2.97	0.0010	2.662	2.70	0.963

N—number of the basin's evolution stage (it corresponds to N in Table 1); $\varphi(0)$—average rock porosity within the near-surface layer at the depth of 0–200 m; b—scale for porosity change versus depth in the law: $(\varphi(z)=\varphi(0)\exp(-z/B))$; K_m—heat conductivity of the matrix rocks at the temperature $T=0$ °C; Al—temperature coefficient of matrix heat conductivity: $K(T)=K_m/(1+\mathrm{Al}\cdot T(°\mathrm{C}))$; C_v—volume heat conductivity of matrix rocks; ρ_m—density of matrix rocks; A—heat generation per unit volume.
Values in this table were computed according to relative content of facies in Table 1 and parameters in Table 3.

admixture of halite and anhydrite (see Table 1, for example). Petrophysical characteristics of the rock mixture (Table 1) including matrix density, heat conductivity, heat capacity, heat generation, and compaction parameters (Table 2) are computed by using the algorithms described in Makhous et al. (1997) and the world average data for the main lithological units of the region presented in Table 3.

In the modeling, variation in heat conductivity with depth and time is determined by depth change of lithology, porosity and temperature of the rock. The later is due to dependence of the matrix and water conductivities on rock temperature (Table 2; Makhous et al., 1997). Fig. 3a demonstrates an example of depth variation in heat conductivity, calculated for present-day sedimentary section of the Akhmerova well. It can be seen that the rocks of the Upper Vendian with a maximal sandy fraction (Table 1) are characterized by maximal conductivity. The decrease of sediment's heat conductivity with increasing of porosity toward surface is considerable for depths of less than 6 km, whereas observed little diminution of conductivity at depths of more than 6 km is caused by temperature dependence of matrix conductivity (Table 2). The computed heat conductivity ranges within the limits ($K=0.9$–4.68 W/m K for limestones, 1.63–6.81 W/m K for sandstones and 0.66–2.80 W/m K for argillite) determined by measurements for sedimentary rocks in the East European Platform and the Ural Foredeep (Salnikov, 1984; Salnikov and Golovanova, 1990; Kukkonen et al., 1997).

Fig. 3b demonstrates depth variations in volume heat generation caused by change in the rock lithology and porosity on an example of the present-day sedimentary section of the Akhmerova well. The Middle Riphean rocks characterized by a maximal content of clay fraction have maximal volume heat generation. Volume heat generation used in our modeling is based on the data of Table 3 for the main lithological units. It ranges within the limits determined by measurements in the sedimentary rocks of the EEP and the Ural Foredeep [$A=0.62$–0.77 mkW/m^3 (Salnikov, 1984) and 0.56 ± 0.52 mkW/m^3 (Kukkonen et al., 1997) for limestones; 1.50–1.83 mkW/m^3 (Salnikov, 1984) for clays; 0.3 mkW/m^3 (Salnikov, 1984) and 0.08 ± 0.05 mkW/m^3 (Kukkonen et al., 1997) for gypsum, anhydrite; 1.00 ± 0.34 mkW/m^3 (Kukkonen et al., 1997) for sandstone]. The average heat generation for the Riphean rocks of the Akhmerov section (0.99 mkW/m^3 in Fig. 3b) differs from the estimation in Salnikov (1984) (1.27 mkW/m^3) by about 30%. Averaged value

Table 3
World average petrophysical parameters of some sedimentary rocks (Sclater and Christie, 1980; Doligez et al., 1986; Burrus and Andebert, 1990; Ungerer et al., 1990; Midttomme and Roaldset, 1999)

N	Rock	$\varphi(0)$	b (km)	K_o (W/m °C)	Al (°C^{-1})	C_v (Mj/m^3 °K)	ρ_o (g/cm^3)	A (μW/m^3)
1	Shale	0.70	1.80	2.09	0.0005	2.26	2.70	2.09
2	Sandstone	0.40	3.00	5.44	0.0030	2.89	2.65	0.84
3	Limestone	0.60	1.90	2.97	0.0005	2.72	2.71	0.63
4	Anhydrite	0.35	0.90	5.44	0.0050	2.01	2.40	0.08

The parameters $\varphi(0)$, b, K_o, Al, C_v, ρ_o and A have the same meaning as in Table 2.

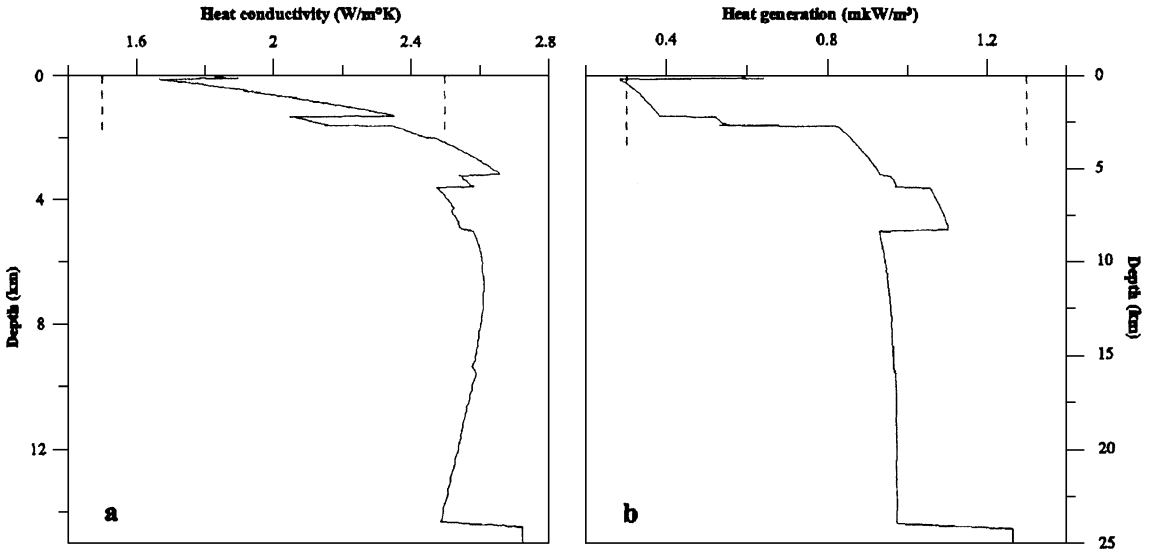

Fig. 3. Calculated variations in heat conductivity (a) and radiogenic heat generation (b) with depth in the present-day sedimentary section of the well Akhmerova. The measured values for rocks in the region range between dotted lines (see text).

for the whole sedimentary section of the Akhmerova well amounts to 0.95 mkW/m^3 (Fig. 3b) and is in a rather good agreement with its estimations of 1.12 and 0.98 mkW/m^3 in Salnikov (1984) and Kukkonen et al. (1997), respectively.

According to the seismic and gravity data (Kazantseva and Kamaletdinov, 1986; Avtoneev et al., 1988; Juchlin et al., 1995; Doring et al., 1997; Echler et al., 1997), a standard continental basement (Table 4; Bayer, 1981), is assumed in our model to be beneath the sedimentary cover of the West Bashkirian basins. The parameters of Table 4 are in agreement with estimations of heat conductivity (K) and heat generation (A) in the present basement rocks of the region:

Table 4
Structure of the continental lithosphere and thermophysical parameters of the rocks (Bayer, 1981)

Layer	Granitic		"Basaltic"	Mantle
Depth of the layer base (km)	5.0	15.0	35.0	>35
Density (kg/m^3)	2750	2750	2900	3300
Heat conductivity (W/m K)	2.72	2.72	1.88	$K=f(T)$*
Radiogenic heat production (μW/m^3)	1.26	0.71	0.21	0.004

Dependence K on T is taken from Schatz and Simmons (1972).

$K=2.3–3.3$ W/m K, $A=0.4–1.4$ mkW/m^3 (Kukkonen et al., 1997) and $K=1.53–3.80$ W/m K, $A=1.1–1.5$ mkW/m^3 (Salnikov, 1984; Salnikov and Golovanova, 1990) for granite, and $A=0.17–0.50$ mkW/m^3 (Salnikov, 1984; Salnikov and Golovanova, 1990) for heat generation of "basaltic" rocks. According to Table 4, heat flow due to radiogenic heat generation in the basement (before its extension) amounts to about 18.3 mW/m^2, from which about 17.6 mW/m^2 is due to crust heat generation and 0.69 mW/m^2 is summary heat generation of the mantle rocks at the depth interval of 35–200 km. All of these values are also in agreement with estimation of radiogenic heat flow of the basement in the Bashkirian region by Salnikov (1984) and Kukkonen et al. (1997).

As opposed to previous evaluations of the thermal state of the region, our approach does not use heat flow and mean temperature gradient data for control of modeling, because heat flow and temperature gradient change strongly with depth (see below). Instead of this, the temperature measurements at depths more than 1 km in 30 wells of the study region published in Salnikov and Ogarinov (1977), Salnikov and Popov (1982), Salnikov (1984), Salnikov and Golovanova (1990) and Golovanova (1993) are considered as an important factor to control the reliability of the thermal history reconstructions. All of these

temperatures are rather reliable by stand-time of the bore-holes and hydrological factor that is discussed in a lot of studies (Salnikov and Popov, 1982; Salnikov, 1984; Salnikov and Golovanova, 1990; Golovanova, 1993). Paleo-climate data play a role in our modeling as a condition on upper boundary of the temperature computing domain. We used the data from Frakes (1979) and Velichko (1987) to describe the South Urals paleoclimate from the Carboniferous up to the Cenozoic and the data from Velichko (1987, 1999) for the Cenozoic with detailed analysis for the last 5 Ma. The mean annual temperature in the Proterozoic is assumed to increase linearly from 10 to 16 °C (Fig. 2a) as an appropriate data is absent.

3.3. Thermal history of the basins

The reconstructed burial and thermal histories of the West Bashkiria Rhiphean basins are illustrated in Fig. 2. Here, two examples are shown, the first of which characterizes the western areas of the study region with moderate Riphean subsidence (wells 1–3, 11, 12 in Fig. 1) and the second—the eastern areas with significant Riphean sedimentation (wells 4–10 in Fig. 1). In the latter areas, variations in the basement tectonic subsidence (Fig. 2h) assume cooling of the lithosphere in the Early and partly Middle Riphean from relatively high initial heat flow ($q_o = 60–70$ mW/m^2) and the basement extension of an amplitude $\beta = 1.10–1.30$. Thus, a little subsidence of the crust base in the Early Riphean (MOHO line in Fig. 2i), regardless of the deposition of more than 10 km of sediments, is due to crust extension of an amplitude $\beta \approx 1.20$. On the contrary, in the western part of the study area (wells 1–3, 11, 12 in Fig. 1), the modeling assumes a tectonic setting in the Riphean typical for a flank of continental rift with moderate initial heat flow $q_o = 40–50$ mW/m^2 (Fig. 2c,d,e) without considerable extension of the lithosphere. In the model, the thickness of the lithosphere is determined by intersection of the current temperature–depth profile with the solidus of peridotite with small H_2O content (< 0.2% H_2O; Wyllie, 1979). In the Early Riphean, this thickness reached only 30–70 km in the eastern areas of the study region (Fig. 2i), but it exceeded 200 km in the western areas (Fig. 2e). Further variations in the basement tectonic subsidence are in agreement with the moderate thermal reactivation of the lithosphere in the Middle Riphean, they resulted in erosion of 400–1200 m of the Low Riphean sediments of maximal thickness in the eastern areas (Fig. 2b,f). The next two relatively weak thermal reactivation assumed by the modeling occurred in the Upper Riphean–Vendian and the Cambrian–Devonian, when 200–500 m of sediments could be locally eroded (Fig. 2b,d,f,h). In the time of closing of the Urals paleoocean, shallow water limestones and sandstones (1500–2500 m) were deposited in the region (Table 2; Fig. 2b,f; Aliev et al., 1977; Belokon et al., 1996; Maslov et al., 1997). In the time that subsequently followed up to the present, the lithosphere cooled slowly and reached a quasi-steady thermal regime in the Cenozoic (Fig. 2e,i).

Thus, according to the modeling, the lithosphere of the West Bashkiria was characterized by relatively low-temperature regime during a great time of its evolution. After cooling in the Early Riphean, rather weak thermal reactivation has not led to considerable heating of the lithosphere. In particular, it resulted in a rather limited variation in the depth of the phase transition of pyroxene to garnet peridotite (Fig. 2e,i) and, correspondingly, in small shift (lesser than 300 m.) of the basement surface caused by the phase transition. Surface heat flow decreased from higher values in the Early Riphean (60–70 mW/m^2 in the eastern areas and 40–50 mW/m^2 in the western) to present-day values of 32–40 mW/m^2 (Fig. 2c,g). The contribution of the radiogenic heat production in the sediments, amounted to about 5–7 mW/m^2 in the present-day section, could explain a main part of the difference between heat flows through the sediment and basement surfaces in Fig. 2c,g. Slight increase of heat flow at the last 2–3 Ma in these figures is a result of a considerable decrease of average annual temperatures (Fig. 2a).

Calculated burial and thermal histories of sedimentary blanket along the two profiles in Fig. 1 are demonstrated in Fig. 4. For discussion, we believe it useful to show, in addition to isotherms, isolines of vitrinte reflectance too, as a control factor of maturity and integral thermal history of buried organic matter in sediments. Although vitrinite is absent in the Riphean and Vendian sediments, we utilized the calculations of vitrinite reflectance as a common method to assess the maturation of organic matter. Vitrinite reflectance (%Ro) is computed by using of the vitrinite kinetic

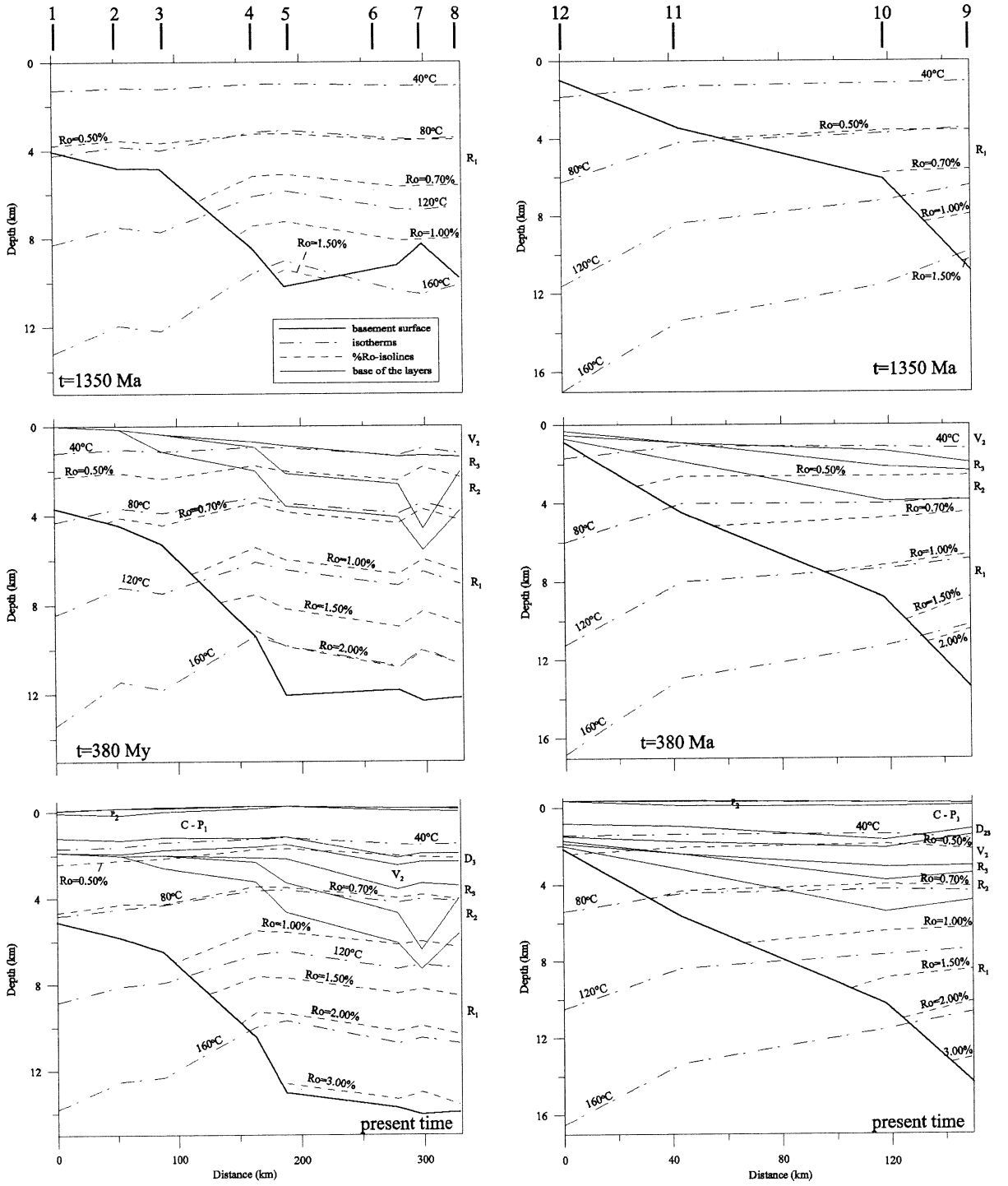

Fig. 4. Numerical reconstruction of burial, thermal and maturation histories of the West Bashkirian sedimentary basins along the profiles 1 and 2 in Fig. 1. Location of the wells are shown by numbers from above. The wells' numbers correspond to the numbers in Fig. 1.

spectrum from Sweeney and Burnham (1990) and thermal history of the strata calculated in the modeling. The algorithm is described in detail in Makhous et al. (1997) and Galushkin (1997). The modeling shows that quite in the Early Riphean the deepest sediments could reach temperature of 150–160 °C and occur within the main zone of liquid hydrocarbons generation ($0.70 \le R_o \le 1.30\%$; Fig. 4). In spite of the relatively low temperature regime of the basin as a whole, a syn-rifting deposition of more than 10 km of limestone, shale and sandstone in the Riphean led to increasing of the present-day temperatures at the base of the sedimentary blanket in the eastern areas up to 180–190 °C (Figs. 2b and 4). The modeling suggests that the sediments at depths of more than 10 km in the present-day section are able to generate dry gas ($R_o \ge 1.50\%$). In the western areas with little syn-rifting subsidence of the basement, temperature of the Riphean sediments does not exceed 120 °C (Fig. 2b) and even drops to 60 °C in the Morozov area (Fig. 4). According to the modeling, the Vendian, Upper and even Middle Riphean deposits must be characterized by relatively low level of organic matter maturity in all of the region. This conclusion is confirmed by few results of geochemical analysis in the region (Belokon et al., 1996; Masagutov et al., 1997; Galushkin et al., 2004).

3.4. Present-day thermal regime of the basins and climate factor

Consideration of the recent climate variations is necessary to compare correctly the measured and calculated temperatures in the region (Kukkonen et al., 1997). We use the climate data from Velichko (1987, 1999) with detailed analysis for the last 1–3 My and incorporate a special supplementary block of the GALO package (Galushkin, 1997) into the numerical simulation of the basin thermal evolution during the Pliocene–Holocene, when the formation and degradation of permafrost took place repeatedly. Some details of our consideration are presented in Appendix A.

Fig. 5 illustrates the result of permafrost modeling on examples of the Morozovskaya area with minimal thickness of the sedimentary blanket in profiles and the Yugomashskaya area with mean thickness of sedimentary cover. Curve 1 in Fig. 5 describes the

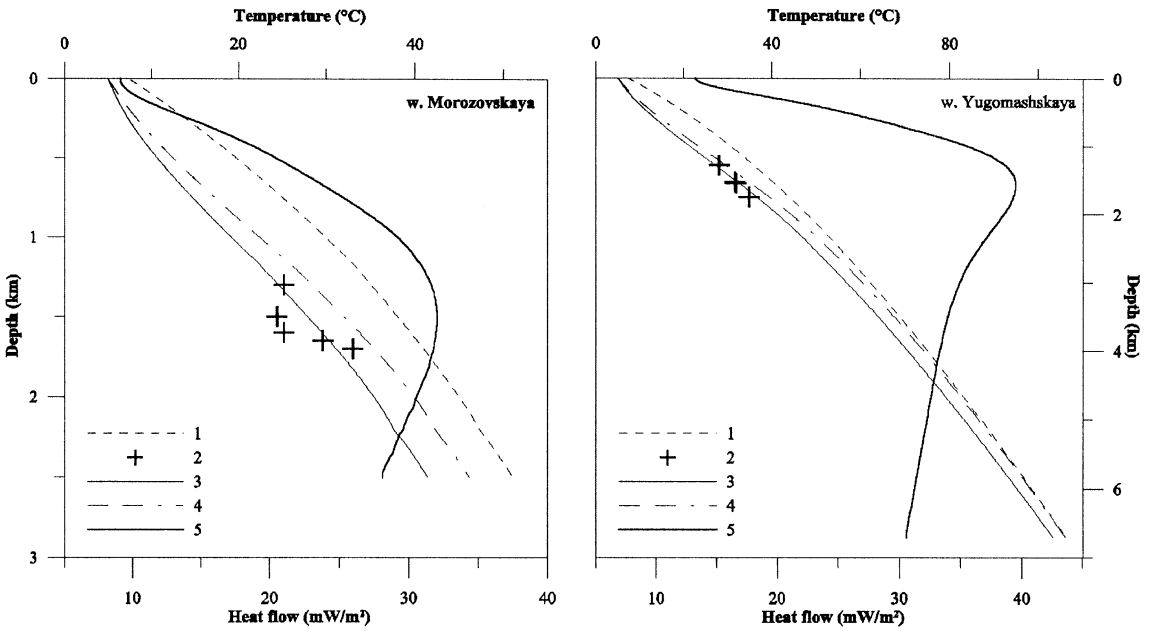

Fig. 5. Temperature and heat flow profiles calculated for the sections of the Morozovskaya and Yugomashskaya wells. 1 = Temperature profile for the time of 4.4 My ago (initial profile for permafrost modeling), 2 = temperatures measured in the present-day section of the areas, 3 = the present-day temperatures, 4 = the present-day temperatures, calculated with climate factor of the last 100,000 years, 5 = calculated present-day heat flow profile.

initial temperature profile computed in the general basin modeling for the age of 4.4 Ma with the climate curve of Fig. 2a generalized for the last 5 My. Curve 3 in Fig. 5a is the present-day temperature distribution computed with consideration of the detail climate variations for last 4.4 My. According to the modeling, the temperature reduction in the upper 2–4 km of the present sedimentary section caused by the last climate factor can reach 10 °C. The curves 4 in Fig. 5 illustrate the present-day temperatures, computed with climate factor of the last 100,000 years. Comparison between the curves 4 and 3 demonstrates the contribution of the climate factor before 100,000 years to formation of the present-day temperature profile. It can reach 5 °C at depths of more than 1.5–2 km. The difference in heat flow is less considerable, and the estimated maximal depth of permafrost for the last glacial age increases approximately by 30 m (375 instead 346 m) due to the climate history before 100,000 years ago.

Calculated variations in the present-day heat flow with depth are shown by curve 5 in Fig. 5. They are typical for all the considered wells in the region. As a result of climatic variations, the heat flow increases quickly in the upper 1–1.2 km, reaches a maximum at depth of 1.5–1.8 km and then decreases gradually to its value at the basement surface. The measurements in the wells of the region confirm such behavior of the heat flow (Kukkonen et al., 1997). These considerations demonstrate that it is necessary to be careful in the modeling based on the measurements of heat flow or temperature gradient at depths of less than 2–2.5 km even in the regions where permafrost has degraded.

3.5. Present-day thermal regime of the mantle in the region

The lines 1 in Fig. 6a,c demonstrate the present-day surface heat flow computed using the climate curve of Fig. 2a. The measured heat flow from Salnikov (1984), Salnikov and Golovanova (1990) and Golovanova (1993) is shown here by stars. These heat flow values are very scattered because the depths of temperature measurements used in the flow assessment differ widely. However, as a whole, it is in reasonable agreement with the calculated values. The calculations confirm the tendency of slightly increase in calculated surface heat flow towards the west boundary of the Urals Folded Zone, noted by V.E. Salnikov (Salnikov, 1984; Salnikov and Golovanova). However, the heat flow through the basement surface (curves 2 in Fig. 6a,c) shows an opposite tendency: it decreases slightly toward the east from 28–32 to 24–26 mW/m^2. The observed discrepancy between curves 1 and 2 in these figures is mainly due to the contribution of radiogenic heat in sediments similarly to

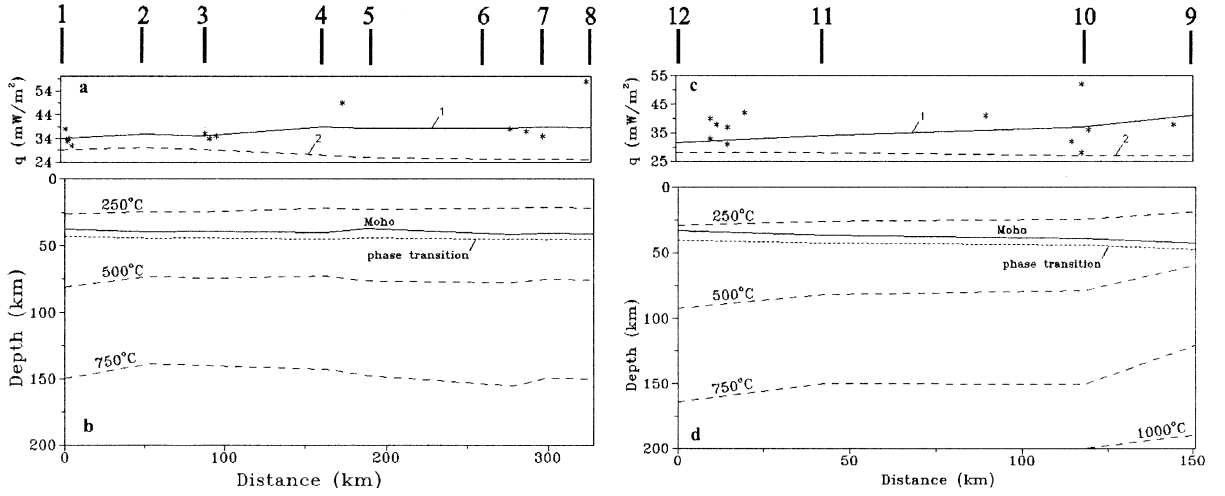

Fig. 6. Present-day heat flow (a, c) and thermal regime of the West Bashkirian lithosphere (b, d) calculated along the profiles 1 and 2. The wells' numbers correspond to the numbers in Fig. 1. In (a, c), lines 1 and 2 denote the heat flow through the sediment and basement surfaces computed with climatic curve of Fig. 2a generalized for the last 4 My (see text). In (b, d), legend is similar to Fig. 2e,i.

Fig. 2c,g. It can be noted that the mantle heat flow obtained by subtraction the radiogenic heat flow of the crust from the basement flow (with consideration of extension of the basin lithosphere with amplitude $\beta = 1.05-1.3$) amounts only 11.3–12.7 mW/m^2, where about 0.6 mW/m^2 is the radiogenic contribution of the mantle rocks. Thus, the estimated mantle heat flow in the region is considerably lesser than the one in usual continental shield amounted 17–25 mW/m^2 (Smirnov, 1980). This is in agreement with the heat flow analysis in Salnikov (1984).

4. Discussion

The analysis of tectonic subsidence, used in our modeling to estimate the duration and the amplitude of the thermal reactivation and stretching events occurring in the history of the West Bashkirian lithosphere, suggests local isostasy of the considered areas (local-isostasy response of the lithosphere on load). The modeling assesses the thermal thickness of the lithosphere (Fig. 2e,i), which is determined by intersection of the thermal curve of the lithosphere and the solidus curve of the mantle rock. However, the state of isostasy is linked to the rheological thickness of the lithosphere. It is known that this state is usually reached when the typical horizontal size of the sediment and water load exceeds considerably the thickness of the effective elastic lithosphere (EEL). Therefore, decrease of the thickness promotes the local isostasy. It was believed early that the lower boundary of EEL is enough deep, coinciding with isotherm of 600–750 °C (Turcotte and Schubert, 1982). Then, the present-day thickness of EEL could amount to 120–150 km in the study region (Fig. 2). Such determination of the EET is valid partly for the oceanic lithosphere, but it is not valid for the continental lithosphere. Recent analysis suggests that the ancient continental lithosphere is considerably weaker than it was thought early (Karter and Tsenn, 1987; Kruse and McNutt, 1988; Lobkovsky, 1988; Burov and Diament, 1995). In Appendix B, we analyze this problem for the present-day low temperature lithosphere of the West Bashkiria. The rheological profiles in Fig. 7 confirm the possibility of considerable weakening even for the low thermal present-day continental lithosphere of the region under consideration, and certainly for the hotter lithosphere of previ-

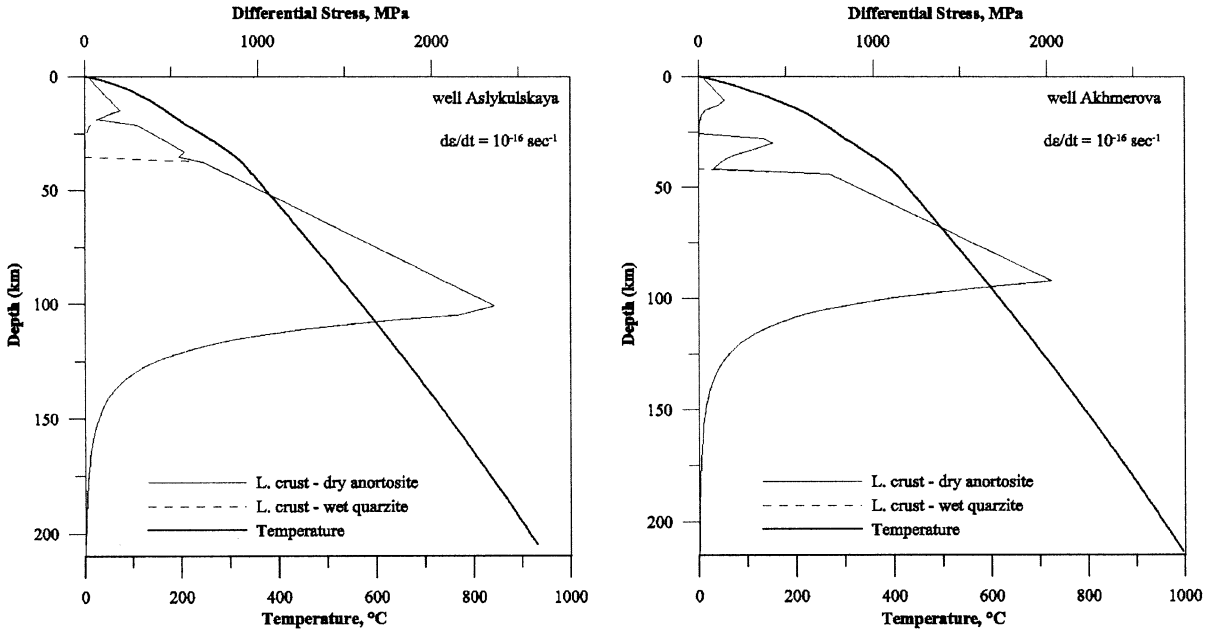

Fig. 7. Yielding strength $\sigma_{xx} - \sigma_{zz}$ of the lithosphere rocks versus depth z calculated from Eqs. (B1)–(B5) for the present-day sections near the wells Aslykulskaya and Akhmerova for strain rate $\dot{\varepsilon} = 10^{-16}$ l/s and reology law discussed in the text.

ous stage of the evolution. This fact is in agreement with the analysis of the Bouguer gravity field along the 1000 km profile across the South Urals (Kruse and McNutt, 1988) suggesting a thickness of 50 km for EEL. At the same time, it is to be noted that the deformations of the elastic plates, quantified in Kruse and McNutt (1988) for the thickness of EEL of 50 and 0 km (the latter corresponds to local isostasy), are close one to another as it can be seen in Fig. 7d of Kruse and McNutt (1988).

Certainly, deviation from the local isostasy can arise during periods of regional compression. But their duration is rather short (10–15 My). After their completion, the state (at least) of regional isostasy will be restored. So, a closing of the Urals paleo-ocean lasted from the Middle Devonian up to the Triassic and was accompanied by deposition of 1500–2500 m of shallow-sea limestones and sandstones in the West Bashkiria. This event was accompanied by the basement tectonic subsidence of 300–800 m in all of the considered areas (Fig. 2d,h). Probably, part of the subsidence could be caused by non-isostatic response of the region lithosphere on the load of the Urals Orogeny in Permian. Then, the erosoin of 200–300 m in the Triassic—the Early Cretaceous could be explained by the relaxation of the lithosphere to an isostatic equilibrium. This equilibrium could be reached at the end of the Early Cretaceous—beginning of the Upper Cretaceous when the movement of the basement surface became minimal (Fig. 2b,d,f,h). The relative low free-air gravity anomalies in the studied region (Artemjev et al., 1994) speak well also for the state close to isostatic equilibrium of the present-day lithosphere in the region.

Analysis of variation in tectonic subsidence of the basement surface suggests several events of thermal reactivation and stretching during the development history of the lithosphere of the West Bashkiria (Fig. 2). The principle of the estimation of duration and amplitude of such events was shortly discussed in Section 3.3 and more detailed in Makhous et al. (1997) and Makhous and Galushkin (2003). Of course, tectonic analysis alone does not give the desirable assessment of these parameters. Indeed, the same sequence of events, but with increased initial and final heat flows in the model, could be in agreement with the same tectonic curve. However, combination of the tectonic method with the control by temperatures measured in boreholes decreases the uncertainty in the modeling procedure and, at the same time, the number of appropriate variants suggested by modeling for basin evolution.

Another problem of modeling could be concerned with the one-dimensional approach in the GALO system. This problem is particularly discussed in our next paper on an example of the present-day thermal state of the region. We carried out a two-dimensional modeling of thermal regime of the lithosphere along the profile 2 (Fig. 1) continuing it to the east across the Tagil–Magnitigorsk Zone of the South Urals. Comparison of the one-dimensional solution with the two-dimensional one for the region studied in this paper showed that deviations from the two-dimensional approach could be considerable only within the Ural Foredeep. Thus, even for the Akhmerova well located within the western margin of the Ural Foredeep, the one-dimensional temperatures differed from those in the two-dimensional variant no more than 5% in all of the depth interval $0 \leq z \leq 200$.

5. Conclusions

Application of the GALO system to numerical reconstruction of burial and thermal histories of the Riphean basins in the West Bashkiria suggests a relatively low-temperature regime of the lithosphere in the region during a great time of its evolution (Figs. 2 and 4). After cooling in the Early Riphean, a rather weak thermal reactivations has not led to considerable heating of the lithosphere. Surface heat flow decreased from higher values in the Early Riphean (60–70 mW/m^2 in the eastern areas and 40–50 mW/m^2 in the western) to present-day values of 32–40 mW/m^2 (Fig. 2). In spite of the relatively low temperature regime of the basin as a whole, a syn-rifting deposition of more than 10 km of limestone, shale and sandstone in the Riphean resulted in rather high temperatures (180–190 °C) at the base of the present-day sedimentary blanket in the eastern areas of the region (Figs. 2b and 4). The modeling suggests that the sediments at depths of more than 10 km in the present-day section of the eastern areas of the region could generate dry gas, whereas the Vendian, Upper and even Middle Riphean locate within the immature zone or in the upper part of

the liquid hydrocarbon zone over all of the region, in spite of very long time of burial (Fig. 4).

In agreement with the observed data, computed present-day heat flow through the sediment surface increases slightly from 32 to 34 mW/m^2 near the west boundary of the region to 42 mW/m^2 near the boundary of the Ural Foldbelt, whereas the heat flow through the basement surface decreases slightly from 28–32 to 24–26 mW/m^2 in the same direction. The mantle heat flow amounts only to 11.3–12.7 mW/m^2, which is considerable lower than mean heat flow of the Russian Platform (16–18 mW/m^2) and is comparable with the low heat flow of Precambrian shields (Smirnov, 1980). Such situation is typical for all of the South Urals, and it could be assumed that it is perhaps related with mantle flow caused by very slow submerging of some parts of the ancient oceanic (or back-arc) plate to the mantle at depths of 300–500 km. Then the flow can stimulate a cooling of the upper mantle. Certainly, this problem needs additional geophysical and geological investigations.

Acknowledgements

We are grateful to the reviewers, Dr. Hi Tim and Dr. Munzer Makhous, for useful discussions and helpful comments, which improved the manuscript.

Appendix A. Some specific features in the modeling of Pliocene–Holocene thermal history for the basins of northern latitudes

The presence of ice in rock pores of sedimentary cover complicates the depth variations of heat conductivity K and heat capacity C_v in the section (Lachenbruch et al., 1982; Galushkin, 1997):

$$K = K_m^{(1-\varphi)} K_w^{\varphi};$$
$$C_v = C_{vm}(1-\varphi) + C_{vw}\varphi \quad \text{for } T > T_l \qquad \text{(A1)}$$

and

$$K = K_m^{(1-\varphi)} K_w^{\varphi W(T)} K_i^{\varphi(1-W(T))};$$
$$C_v = C_{vm}(1-\varphi) + C_{vw}\varphi W(T) + C_{vi}\varphi(1-W(T)) + \rho_L(dW/dT) \quad \text{for } T < T_l \qquad \text{(A2)}$$

Here, K_m, C_{vm}, K_w, C_{vw}, K_i, C_{vi} represent matrix, water and ice heat conductivity and capacity, ρ_L is the latent heat of ice fusion per unit volume, T_l is the liquidus temperature for porous water and $W(T)$ is a fraction of unfrozen water in rock pores. Porosity φ and temperature T in Eqs. (A1) and (A2) are functions of depth z.

Numerical description of the parameters in Eqs. (A1) and (A2), solution algorithm and difference scheme are considered in detail in Galushkin (1997), on an example of the West Siberian Basin. Here, we could note that the main specific feature of modeling of permafrost problem consists in the sharp change (by 1–2 order(s) of magnitude) in the apparent volumetric heat capacity $C_v(2)$ near the base of permafrost caused by rather great value of C_{vi} and sharp change in $W(T)$ near the temperature T_l. The narrow depth interval, within which the main latent heat effect takes place, must include at least 3–4 depth steps, Δz, to ensure reasonable accuracy of the numerical results. In addition, time step Δt must be small enough so that the calculated movement of the freezing front during the time step would be smaller than the corresponding depth step Δz. Thus, in our modeling, the number of depth steps reached 800, and Δz ranged from 0.5 m near the surface to 70 m at the base of the sedimentary column. Time steps Δt varied from 50 to 0.1 years. It should also be noted that, in our modeling, the shape of the $W(T)$ function changes with the depth depending on the content of fine- and coarse-grained fractions in the rock, whereas in paper (Galushkin, 1997), the single function $W(T)$ for coarse sands was utilized, because the rocks in the upper 1–2 km of sedimentary layer in the Urengoy Field are considerably fractured. Consideration of $W(T)$ as a function of rock lithology led to change in estimated depth of permafrost of order of 80 m for the last ice age.

Appendix B. Rheology of continental lithosphere in the study region

The rheological behavior of the continental lithosphere in reference to the present-day low temperature regime of the West Bashkiria is analyzed in Section 4 and in this appendix. The strength for brittle deformation in the continental lithosphere is taken from

Bassi and Bonnin (1988) using the Byerlee's law (Byerlee, 1968) for static friction and variation of rock density with depth from Table 4. Then, brittle strength must increase linearly with depth according to following laws:

$$\sigma_{xx} - \sigma_{zz} = 12.0z + 20 \quad \text{(B1)}$$

–within the sedimentary layer of the continental crust with mean density $\rho \approx 2600$ kg/m^3 ($0 \le z \le S_{sed}$),

$$\sigma_{xx} - \sigma_{zz} = 12S_{sed} + 12.8(z - S_{sed}) + 20. \quad \text{(B2)}$$

–within the granitic layer with density $\rho \approx 2750$ kg/m^3 ($S_{sed} \le z \le S_{sed} + S_{gran}$),

$$\sigma_{xx} - \sigma_{zz} = 12S_{sed} + 12.8(S_{sed} + S_{gran}) + 23.2(z - S_{sed} - S_{gran}) + 20. \quad \text{(B3)}$$

–within the "basaltic" layer with $\rho \approx 2900$ kg/m^3 ($S_{sed} + S_{gran} \le z \le S_{MOHO}$), and

$$\sigma_{xx} - \sigma_{zz} = 12S_{sed} + 12.8(S_{sed} + S_{gran}) + 23.2(S_{MOHO} - S_{sed} - S_{gran}) + 26.4(z - S_{MOHO}) + 20. \quad \text{(B4)}$$

in the mantle with $\rho \approx 3300$ kg/m^3 ($z \ge S_{MOHO}$). In Eqs. (B1)–(B4), $\sigma_{xx} - \sigma_{zz}$ is the principal stress difference in MPa, S_{sed}, and S_{gran}, S_{MOHO} are the thickness of sedimentary blanket, upper crust (granite layer) and depth of lower boundary of the crust, respectively (in km), z is the depth in km, and 20 MPa is the assumed value of the rock strength at the surface (Byerlee, 1968). The (B1)–(B4) for brittle deformation assume that the pore pressure is hydrostatic within the upper continental crust and equal to zero within the lower crust and the mantle (Brace and Kohlstedt, 1980; Thibaud et al., 1999).

The strength for ductile (creep) deformation in the crust and mantle is described by the power-law (Brace and Kohlstedt, 1980; Kirby, 1983):

$$\sigma_{xx} - \sigma_{zz} = (\dot{\varepsilon}/A)^{1/n} \exp[E/nRT] \quad \text{(B5)}$$

where $\dot{\varepsilon}$ is the deformation rate in l/s, $(\sigma_{xx} - \sigma_{zz})$ is in MPa, E is the activation energy for the ductile deformation in J/mol, $R = 8.31441$ J/mol K is the universal gas constant, T is the absolute temperature, A is a material constant in MPa^{-n} s^{-1}, and n is a dimensionless parameter. Values of parameters E, A and n depend on the mineral types. In our model, the rheology of wet quartz with parameters $A = 0.00291$ MPa^{-n} s^{-1}, $E = 151$ KJ/mol and $n = 1.8$ (Jaoul et al., 1984; Ord and Hobbs, 1989) describes a behavior of the continental upper crust. At the temperature range of 200–700 °C, it is very close to the rheology of wet granite with parameters $A = 0.0002$ MPa^{-n} s^{-1}, $E = 137$ KJ/mol and $n = 1.9$ (Kirby, 1983; Meissner and Kusznir, 1987; Ord and Hobbs, 1989). The rheology of the lower continental crust is assumed to correspond to that of dry anortosite with the following parameters: $A = 3.27 \times 10^{-4}$ MPa^{-n} s^{-1}, $E = 239$ KJ/mol and $n = 3.2$ (Shelton and Tullis, 1981; Ranalli and Murphy, 1987; Ord and Hobbs, 1989; Takeshita and Yamaji, 1990). At temperatures T>500 °C, this rheology is close to that of dry quartz (Jaoul et al., 1984) with parameters $A = 3.44 \times 10^{-6}$ MPa^{-n} s^{-1}, $E = 184$ KJ/mol and $n = 2.8$. And finally, the rheological behavior of the mantle material is described in our model by the deformation law (B5) with the parameters for dry dunite ($A = 2.88 \times 10^4$ MPa^{-n} sec^{-1}, $E = 535$ KJ/mol and $n = 3.6$). They are taken from Chopra and Paterson (1981, 1984), in which the temperature control of deformation experiments is, perhaps, the most reliable (Ord and Hobbs, 1989).

The distribution of the rock strength with depth is inferred then by choice of the minimal value among the stress differences, calculated by Eqs. (B1)–(B5) for the given depth (Ranalli and Murphy, 1987; Ord and Hobbs, 1989). Fig. 7 demonstrates the calculated distribution of yielding strength with depth in the West Bashkirian region on an example of the present-day sections in two areas: Aslykulskaya and Akhmerova. The calculations are carried out for the strain rate $\dot{\varepsilon} = 10^{-16}$ l/s, which is expected to be typical for stable continental areas (Takeshita and Yamaji, 1990) and characterizes greater part of the region history excluding perhaps the relative short times close to rifting or the stage of Urals Orogeny. For comparison, the profiles with wet quartzite rheology for all the continental crust considered in many paeres (Brace and Kohlstedt, 1980; Kirby, 1983; Ord and Hobbs, 1989; Ranalli, 2000) are shown in these figures by dotted lines. Fig. 7 shows considerable weakening of the mantle lithosphere at depths of below 90–110 km even for the low-temperature,

present-day regime of the West Bashkirian lithosphere. For the rheology of wet quartzite for all the crust, ductile zone occupies all of the lower crust even in the western section of the region (Fig. 7). Stress profiles in Fig. 7 demonstrate clearly considerable weakening of the crust due to deposition of thick sedimentary cover (compare Fig. 7b and a). This effect relates mainly with increase in rock temperature within the crust under the cover. This fact explains, to some extent, a readiness of thick sedimentary basins for tectonic remobilization (the East Barents basin, West Siberia basin and others). At significant deposition, ductile zone appears at the base of the granite layer too (Fig. 7b). In any case, the modeling results in Fig. 7 suggest that the rheological thickness of the lithosphere must be considerably lesser than its thermal thickness exceeding in the region 200 km. Reactivation of existing faults during restoration of isostasy state of the lithosphere increased the above difference (Ranalli, 2000).

References

Aliev, M.M., Morozov, S.G., Postnikova, I.E., 1977. Geology and oil–gas prospecting of the Riphean and Vendian deposits in the Volga–Urals region. Nedra, Moscow. 156 pp. (in Russian).

Artemjev, M.E., Kaban, M.K., Kucherenko, V.A., Demyanov, G.V., Taranov, V.A., 1994. Subcrustal density inhomogeneities of northern Eurasia as derived from the gravity data and isostatic models of the lithosphere. Tectonophysics 240, 249–280.

Avtoneev, V., Druzhinin, V.S., Kashubin, N., 1988. Deep structure of the South Urals along the Troitsk profile DSZ. Sov. Geol. 7, 47–57 (in Russian).

Bassi, G., Bonnin, J., 1988. Rheological modeling and deformation instability of lithosphere under extension—II. Depth-dependent rheology. Geophys. J. 94, 559–565.

Bayer, A.J., 1981. Geothermal evolution of the lithosphere and plate tectonics. Tectonophysics 72, 203–227.

Belokon, T.V., Balashova, M.M, Gorbachov, V.I., Sirotenko, O.I., Denisov, A.I., 1996. Prospect of the Riphean and Vendian deposits in the eastern Russian platform. Geologiya, metody poiskov, razvedki i otsenki mestorozhdeniy toplivno-energeticheskogo seria, Obzor. AOZG "Geoinformmark", Moscow. 38 pp. (in Russian).

Brace, W.F., Kohlstedt, D.L., 1980. Limits on lithospheric stress imposed by laboratory experiments. J. Geophys. Res. 85 (B11), 6248–6252.

Burov, E.B., Diament, M., 1995. The effective elastic thickness (Te) of continental lithosphere: what does it really mean? J. Geophys. Res. 100, 3905–3927.

Burrus, J., Andebert, F., 1990. Thermal and compaction processes in a young rifted basin containing evaporites: gulf of Lions, France. AAPG Bull. 74, 1420–1440.

Byerlee, J.D., 1968. Brittle–ductile transition in rocks. J. Geophys. Res. 73, 4741–4750.

Chopra, P.N., Paterson, M.S., 1981. The experimental deformation of dunite. Tectonophysics 78, 453–473.

Chopra, P.N., Paterson, M.S., 1984. The role of water in the deformation of dunite. J. Geophys. Res. 89, 7861–7876.

Didenko, A.N., Kurenkov, S.A., Ruzhentsev, S.V., Simonov, V.A., Lubnina, N.V., Kuznetsov, N.B., Aristov, V.A., Borisenok, D.V., 2001. Tectonic history of the Polar Urals. Nauka, Moscow. 192 pp. (in Russian).

Doligez, B., Bessis, F., Burrus, J., Ungerer, P., Chenet, P.Y., 1986. Integrated numerical simulation of the sedimentation heat transfer, hydrocarbon formation and fluid migration in a sedimentary basin. The THEMIS model. In: Burrus, J. (Ed.), Thermal Modelling in Sedimentary Basins. Editions Technip, Paris, pp. 173–195.

Doring, J., Gotze, H.-J., Kaban, M.K., 1997. Preliminary study of the gravity field of the southern Urals along URSEIS '95 seismic profile. Tectonophysics 276, 49–62.

Echler, H.P., Ivanov, K.S., Ronkin, Y.I., Karsten, L.A., Hetzel, R., Noskov, A.G., 1997. The paleozoic tectono–metamorphic evolution of gneiss complexes in the Middle Urals: a reappraisal. Tectonophysics 276, 229–251.

Forsyth, D.W., Press, F., 1971. Geophysical tests of petrological models of the spreading lithosphere. J. Geophys. Res. 76, 7963–7972.

Frakes, L.A., 1979. Climates Throughout Geological Time. Elsevier, Amsterdam, pp. 1–310.

Frolovich, G.M., Khachatryan, R.O., Goldobin, Yu.P., 1988. Structure of northern part of the Kama-Belsk basin from seismology data. Izv. AN SSSR. Ser. Geol. 10, 126–136 (in Russian).

Galushkin, Yu.I., 1997. Numerical simulation of permafrost evolution as a part of basin modeling: permafrost in Pliocene–Holocene climate history of Urengoy field in West Siberian basin. Can. J. Earth Sci. 34, 935–948.

Galushkin, Yu.I., Simonenkova, O.I., Lopatin, N.V., 1999. Thermal and maturation modelling of Urengoy field, the West Siberian Basin: some peculiarities in basin modeling. AAPG Bull. 83, 1965–1979.

Galushkin, Yu.I., Yakovlev, G.E., Kuprin, V.F., 2004. Catagenesis evolution and realization of the potential for hydrocarbon generation by organic matter in the Riphean and Vendian deposits of the West Bashkirian basins: numerical modeling. Geochimiya 1 (in Russian).

Golovanova, I.V., 1993. Heat flow of he South Urals and its relation with tectonics. In: Kononov, B.I., Yudachin, F.N., Svalova, V.B. (Eds.), Geothermal Studies of Seismic and Aseismic Zone. Nauka, Moscow, pp. 48–55 (in Russian).

Jaoul, O., Tullis, J., Kronenberg, A.K., 1984. The effect of varying water contents on the creep behaviour of heavitree quartzite. J. Geophys. Res. 89, 4298–4312.

Juchlin, C., Kashubin, S., Knapp, J.H., Makovsky, V., Ryberg, T., 1995. Project conducts seismic reflection profiling in the Urals Mountains. Trans. Am. Geophys. Union, EOS 76 (19), 193–197.

Karter, N., Tsenn, M.C., 1987. Flow properties of continental lithosphere. Tectonophysics 136, 27–63.

Kazantseva, K.K., Kamaletdinov, M.A., 1986. The geossynclinal development of the Urals. Tectonophysics 127, 371–381.

Khutorskoy, M.D., Abizgildin, I.Kh., Paduchikh, V.I., 1993. Heat flow in the Mugodgary—continuation of the South Urals geothermal anomaly. In: Kononov, V.I., Yudakhin, F.N., Svalova, V.B. (Eds.), Geotermia Seismichnykh I Aseismichnykh Zon. Nauka, Moscow, pp. 55–70 (in Russian).

Kirby, S.H., 1983. Rheology of the lithosphere. Rev. Geophys. Space Phys. 21, 1458–1487.

Kruse, S., McNutt, M., 1988. Compensation of Paleozoic orogens: comparison of the Urals to the Appalachians. Tectonophysics 154, 1–17.

Kukkonen, I.T., Golovanova, I.V., Khachay, Yu.V., Druzhinin, V.S., Kosarev, A.M., Schapov, V.A., 1997. Low geothermal heat flow of the Urals fold belt—implication of low heat production, fluid circulation or paleoclimate? Tectonophysics 276, 63–85.

Lachenbruch, A.H., Sass, J.H., Marshall, B.V., Moses, T.H., 1982. Permafrost, heat flow and the geothermal regime at Prudhoe Bay, Alaska. J. Geophys. Res. 87, 9301–9316.

Lobkovsky, L.I., 1988. Geodynamics of Spreading Zones, Subduction, and Two-Level Plate Tectonics Nauka, Moscow. 252 pp. (in Russian).

Makhous, M., Galushkin, Yu.I., 2003. Burial history and thermal evolution of the lithosphere of the northern and eastern Saharan Basins. AAPG Bull. 87 (10), 1623–1651.

Makhous, M., Galushkin, Yu.I., Lopatin, N.V., 1997. Burial history and kinetic modeling for hydrocarbon generation: Part I. The GALO Model. AAPG Bull. 81 (10), 1660–1678.

Masagutov, R.H., Kozlov, V.I., Andreev, Yu.V., Ivanova, T.V., 1997. Prospect of the Riphean and Vendian deposits in the western Bashkirian. Gelogia, Geophysika and Razrabotka Neftyanych Mestorozhdeniy N.1, 2–9; N.7, 2–7; N.9, 2–7 (in Russian).

Maslov, A.V., Erdtmann, B.-D., Ivanov, K.S., Ivanov, S.N., Krupenin, M.T., 1997. The main tectonic events, depositional history, and the paleogeography of the southern Urals during the Riphenian–Early Paleozoic. Tectonophysics, 313–335.

Meissner, R., Kusznir, N.J., 1987. Crustal viscosity and the reflectivity of the lower crust. Ann. Geophys. 5B (4), 365–374.

Midttomme, K., Roaldset, E., 1999. Thermal conductivity of sedimentary rocks: uncertainties in measurement and modeling. In: Aplin, A.C., Fleet, A.J., Macquaker, J.H.S. (Eds.), Mud and Mudstones: Physical and Fluid Flow Properties. Geol. Soc. London, Spec. Publ., vol. 158, pp. 45–60.

Ord, A., Hobbs, B.E., 1989. The strength of the continental crust, detachment zones and the development of plastic instabilities. Tectonophysics 158, 269–289.

Ranalli, G., 2000. Rheology of the crust and its role in tectonic reactivation. J. Geodynamics 30, 3–15.

Ranalli, G., Murphy, D.C., 1987. Rheological stratification of the lithosphere. Tectonophysics 132, 281–295.

Ruzhenzev, S.V., 1976. Marginal Ophiolitic Allochtones (Structure and Tectonic Origin). Nauka, Moscow. 171 pp. (in Russian).

Salnikov, V.E., 1984. Geothermal Regime of the South Urals. Nauka, Moskow. 88 pp. (in Russian).

Salnikov, V.E., Golovanova, I.V., 1990. New data on the heat flow distribution in the South Urals. Geol. Geophys. 12, 129–135 (in Russian).

Salnikov, V.E., Ogarinov, I.S., 1977. The South Urals Zone of anomalous low heat flow. Dokl. Akad. Nauk SSSR 273, 1456–1459 (in Russian).

Salnikov, V.E., Popov, V.G., 1982. Geothermal regime and geodynamics of the South Urals and nearest areas. Izv. Akad. Nauk SSR, Ser. Geol. 3, 128–135 (in Russian).

Schatz, J.F., Simmons, G., 1972. Thermal conductivity of Earth materials at high temperatures. J. Geophys. Res. 77 (35), 6966–6983.

Sclater, J.G., Christie, P.A.F., 1980. Continental stretching: an explanation of the post-mid Cretaceous subsidence of the central North sea basin. J. Geophys. Res. 85, 3711–3739.

Shelton, G., Tullis, J., 1981. Experimental flow laws for crustal rocks: EOS. Trans. Am. Geophys. Union 62, 396.

Smirnov, Ya.B., 1980. Heat flow in USSR: remarks to the heat flow and deep temperatures maps in the scale 1:10,000,000 GUGK, Moscow. 150 pp. (in Russian).

Sweeney, J.J., Burnham, A.K., 1990. Evolution of a simple model of vitrinite reflectance based on chemical kinetics. AAPG Bull. 74, 1559–1570.

Takeshita, T., Yamaji, A., 1990. Acceleration of continental rifting due to a thermomechanical instability. Tectonophysics 181, 307–320.

Thibaud, R., Dauteuil, O., Gente, P., 1999. Faulting pattern along slow-spreading ridge segments: a consequence of along-axis variation in lithospheric rheology. Tectonophysics 312, 157–174.

Turcotte, D.L., Schubert, G., 1982. Geodynamics. Wiley, New York. 374 pp.

Ungerer, P., Burrus, I., Doligez, B., Chenet, P., Bessis, F., 1990. Basin evolution by integrated two-dimensional modeling of heat transfer, fluid flow, hydrocarbon generation, and migration. AAPG Bull. 74, 309–335.

Velichko, A.A., 1987. Climatic variations in Meso–Cenozoic by the data for East Europe. Climates of the Earth in Geological History. Nauka, Moscow, pp. 5–43 (in Russian).

Velichko, A.A. (Ed.), 1999. The Climate and Landscape During the Last 65 Ma (Cenozoic: from Paleocene to Holocene). GEOS, Moscow. 260 pp. (in Russian).

Welte, D.H., Horsfield, B., Baker, D.R. (Eds.), 1997. Petroleum and Basin Evolution. Springer-Verlag, Berlin. 536 pp.

Working Scheme on Stratigraphy and Correlation of Upper Proterozoic in West Bashkiria, 1981. Ufa. 35 pp. (in Russian).

Wyllie, P.J., 1979. Magmas and volatile components. Am. Mineral. 64, 469–500.